

Deuterium depth profiling in JT-60U tiles using the $D(^3\text{He}, p)^4\text{He}$ resonant nuclear reaction

T. Hayashi ^{a,*}, K. Sugiyama ^b, K. Krieger ^c, M. Mayer ^c, V.Kh. Alimov ^d,
T. Tanabe ^b, K. Masaki ^a, N. Miya ^a

^a Japan Atomic Energy Agency, Mukoyama 801-1, Naka, Ibaraki 311-0193, Japan

^b Interdisciplinary Graduate School of Engineering Sciences, Kyushu University, Hakozaki 6-10-1, Higashi-ku, Fukuoka 812-8581, Japan

^c Max-Planck-Institut für Plasmaphysik, EURATOM Association, Boltzmannstrasse 2, D-85748 Garching, Germany

^d Institute of Physical Chemistry of the Russian Academy of Sciences, Leninskii prospekt 31, 117915 Moscow, Russian Federation

Abstract

Deuterium depth profiles in graphite tiles of JT-60U have been determined by means of the $D(^3\text{He}, p)^4\text{He}$ nuclear reaction. Tiles with net carbon deposition showed high deuterium retention. A D/C ratio of 0.07 was found in the outer dome wing tile. In the inner divertor tile covered with a thick deposition layer, the depth profile shows a broad peak in a deep region. This indicates that deuterium trapped in the shallow region can be replaced by hydrogen with hydrogen discharges due to isotope exchange, while deuterium trapped in the deeper region can not. Deuterium in the redeposited layers can be more easily removed than that in the substrate. The deuterium concentration in the outer divertor target tile was very low ($D/C < 0.003$). The highest D/C ratio, 0.09, was found in the upper region of the first wall.

© 2007 Elsevier B.V. All rights reserved.

PACS: 28.52.Fa; 28.52.Nh; 52.40.Hf; 52.55.Fa

Keywords: Deuterium inventory; Carbon-based material; First-wall; JT-60U; Surface analysis

1. Introduction

Tritium (T) and deuterium (D) are used as fuels for a fusion reactor. A significant fraction of tritium is retained both on the surface and inside of the plasma-facing materials. For radiological safety, one of the most important outstanding issues is to understand tritium behavior and to predict the tri-

tium inventory of in-vessel components. Much research regarding tokamak experimental device plasma-wall interaction and erosion/deposition has been reported [1–4]. In the JAERI Tokamak-60 Upgrade (JT-60U), deuterium discharges have been carried out. In order to estimate the tritium retention in future tokamak reactors including ITER, it is very important to investigate the retention characteristics of deuterium in carbon tiles used in JT-60U.

Recently, detailed analyses of deuterium and hydrogen in plasma-facing graphite tiles of JT-60U

* Corresponding author.

E-mail address: hayashi.takao@jaea.go.jp (T. Hayashi).

have been performed using secondary ion mass spectroscopy (SIMS), thermal desorption spectroscopy (TDS), a nuclear reaction analysis (NRA) and a scanning electron microscope (SEM) [5–8]. Although the SIMS analysis gives depth profiles of hydrogen isotopes together with impurities, it is hard to give quantitative concentrations. In a previous work [6], we have performed a quantitative NRA analysis of deuterium retained in the graphite tiles used in JT-60U using a 350 keV deuterium beam. The depth profile given by the 350 keV beam was limited within 2 μm from the surface, which was not thick enough to discuss deuterium retention in detail. Therefore, the deuterium depth profile in deeper regions should be investigated in order to understand the plasma–wall interaction in more detail.

In this paper, we have made a quantitative depth analysis of deuterium in plasma-facing graphite tiles used in JT-60U by means of the $\text{D}({}^3\text{He}, \text{p}){}^4\text{He}$ resonant nuclear reaction. The maximum depth which can be analyzed is about 14×10^{23} carbon atoms/ m^2 corresponding to 16 μm for graphite of 1.7 g/cm^3 .

2. Experimental

2.1. Samples

Fig. 1(a) and (b) shows the poloidal locations of analyzed samples in the cross sections of (a) JT-60U and (b) the W-shaped divertor. Carbon fiber composite (CFC) materials were used for the divertor target tiles (ID and OD) and the dome top tile (DM1). All other tiles were made of isotropic fine grain graphite. Samples of the first wall were referred as original addresses of the JT-60U plasma facing tiles. The operational temperature of the vac-

uum vessel was ~ 570 K. The first wall tiles shown in Fig. 1(a) were exposed to plasma from March 1991 to October 1999. The divertor targets and the dome tiles shown in Fig. 1(b) were exposed from March 1997 to October 1998.

In the operation period from June 1997 to October 1998, about 4300 pulse discharge experiments (~ 3600 deuterium discharges and ~ 700 hydrogen discharges) were carried out with the W-shaped divertor configurations. Plasma in the inner-private flux region was pumped through a full toroidal inner slot. After a deuterium discharge period, hydrogen discharges were carried out to reduce tritium produced by DD reactions and retained in the vessel wall.

The temperature of the outer strike point (OD) was higher than that of the inner strike point (ID). The maximum surface temperatures of the outer and the inner divertor tiles were estimated from the bulk temperature measured by thermocouples embedded at a depth of 6 mm to be ~ 1400 K and ~ 1000 K, respectively [6]. The maximum surface temperature of the dome region (DM1 and DM2) was estimated to be ~ 800 K.

2.2. Nuclear reaction analysis (NRA)

Deuterium depth profiles were determined by using the $\text{D}({}^3\text{He}, \text{p}){}^4\text{He}$ resonant nuclear reaction. Because the cross section of the $\text{D}({}^3\text{He}, \text{p}){}^4\text{He}$ nuclear reaction has a broad resonant peak at a ${}^3\text{He}$ energy of about 0.6 MeV, the deuterium depth profiles can be obtained by varying the incident energy of the ${}^3\text{He}$ beam. The ${}^3\text{He}$ beam at energies from 0.8 to 3.5 MeV was produced by a 3 MV tandem accelerator at IPP Garching, Germany. Samples with a size of $10 \times 10 \times 1$ mm^3 were cut from the tiles and were used for ion beam analysis. The beam spot area and beam current were $\sim 1 \times 1$ mm^2 and 0.015–0.05 μA , respectively. Protons produced in the range of 0.5–2 μC were measured at each data point, providing counting statistics for analysis with a statistical error $< 4\%$.

Fig. 2 shows an energy spectrum of charged particles produced by the ${}^3\text{He}$ -induced nuclear reaction for the sample of the outer dome wing tile (DM2). Protons were emitted from the $\text{D}({}^3\text{He}, \text{p}){}^4\text{He}$ nuclear reaction with energies in the range 12.1–13.4 MeV, depending on the incident ${}^3\text{He}$ energy, and were detected using a large-angle detector. A silicon surface-barrier detector with a depletion depth of 1.5 mm was located at a laboratory angle

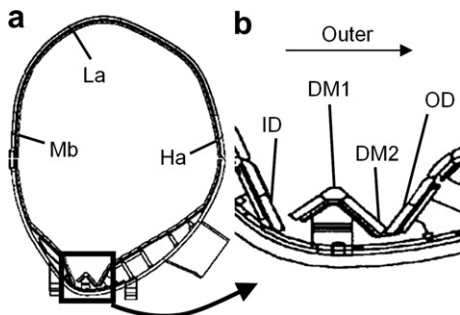


Fig. 1. Poloidal locations of analyzed samples for NRA in poloidal cross sections of (a) the vacuum vessel of JT-60U and (b) the W-shaped divertor.

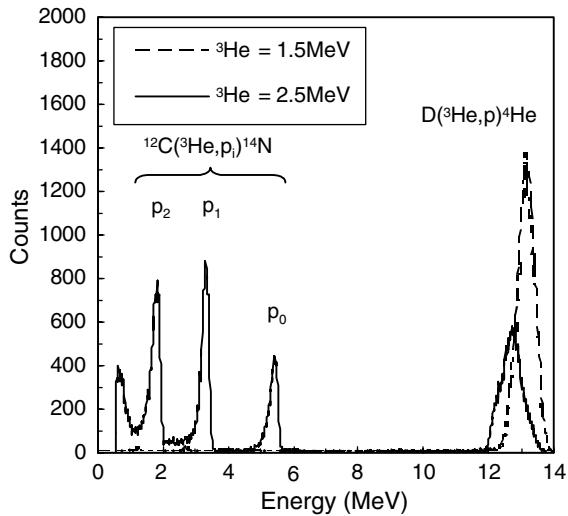


Fig. 2. Charged-particle energy spectra from the ^3He -induced nuclear reaction on the outer dome wing tile sample (DM2).

$\theta = 135^\circ$ with a solid angle of 0.14 sr. A Mylar absorber foil with a thickness of $12\ \mu\text{m}$ was positioned in front of the detector in order to absorb elastically scattered ^3He ions and α particles from the $\text{D}(^3\text{He},\alpha)\text{H}$ nuclear reaction. Highly energetic protons from the $\text{D}(^3\text{He},\text{p})^4\text{He}$ and $^{12}\text{C}(^3\text{He},\text{p}_{0,1,2})^{14}\text{N}$ can reach the detector. In the analysis using a 3.5 MeV ^3He beam, the protons emitted from $^{13}\text{C}(^3\text{He},\text{p}_0)^{15}\text{N}$ nuclear reaction superposed to the peak of the $\text{D}(^3\text{He},\text{p})^4\text{He}$ nuclear reaction. Although ^{13}C was present in the carbon materials with a natural abundance of 1.1 %, we could easily subtract the contribution of ^{13}C as described above.

Deuterium depth profiles were calculated by an iterative method. The first guess profile was made with the SIMNRA [9,10] program, which calculates the proton yield for an energy of the incident ^3He beam. Then, the guess profile was improved, and the calculations repeated until the calculated proton yield as a function of incident ^3He energy agreed with the measured one. We used the detailed cross

section of the $\text{D}(^3\text{He},\text{p})^4\text{He}$ nuclear reaction reported in Ref. [11].

3. Results and discussion

3.1. Contribution of the H-discharge on the formation of the redeposited carbon layers

The ID and DM2 samples were covered by redeposited carbon layers with thickness of $\sim 60\ \mu\text{m}$ and $1\text{--}3\ \mu\text{m}$, respectively [6,12]. Ishimoto et al. [13] have determined the density of the redeposited layers on the inner divertor target tile to be $0.91\ \text{g}/\text{cm}^3$, which is about a half of the density of the tile substrate ($1.7\ \text{g}/\text{cm}^3$) [13]. Consequently, the amounts of carbon deposited on the ID and DM2 were calculated to be 27×10^{23} and $0.45\text{--}1.4 \times 10^{23}$ C atoms/ m^2 , respectively (see Table 1).

In JT-60U, hydrogen discharges were carried out to remove tritium from the plasma-facing wall after the deuterium discharge period. Layers were deposited during the H discharges as well as during D discharges. Assuming the deposition rate being proportional to the injected energy of NBI heating, we estimated the thickness ratio of the redeposited layers made by D-discharges and H-discharges to be ~ 0.03 . It is because the integrated energy injected by NBI during the last H-discharge period before air ventilation is about 3% of the that during the total period of D and H discharges. Hence most of the redeposited layers were produced in the D-discharge period, and the quite surface region of less than 0.8×10^{23} C atoms/ m^2 in the ID sample was the H-deposition layer.

3.2. Deuterium depth profiles in the divertor area

Fig. 3(a) and (b) shows the measured (points) and calculated (lines) proton yields for derivation of D profiles as a function of the applied ^3He energy at (a) the divertor region and (b) the first wall samples. The proton yields were normalized to an analyzing dose of $1\ \mu\text{C}$. Fig. 4(a) and (b) shows

Table 1
Redeposited layer thickness and the analyzed depth

Sample	Location	Redeposited carbon layer		Analyzed depth	
		μm	10^{23} C atoms/ m^2	10^{23} C atoms/ m^2	μm
ID	Inner divertor	60	27	14	30.7
DM2	Outer dome wing	1–3	0.45–1.4	14	17–18
Others	–	0	0	14	16.4

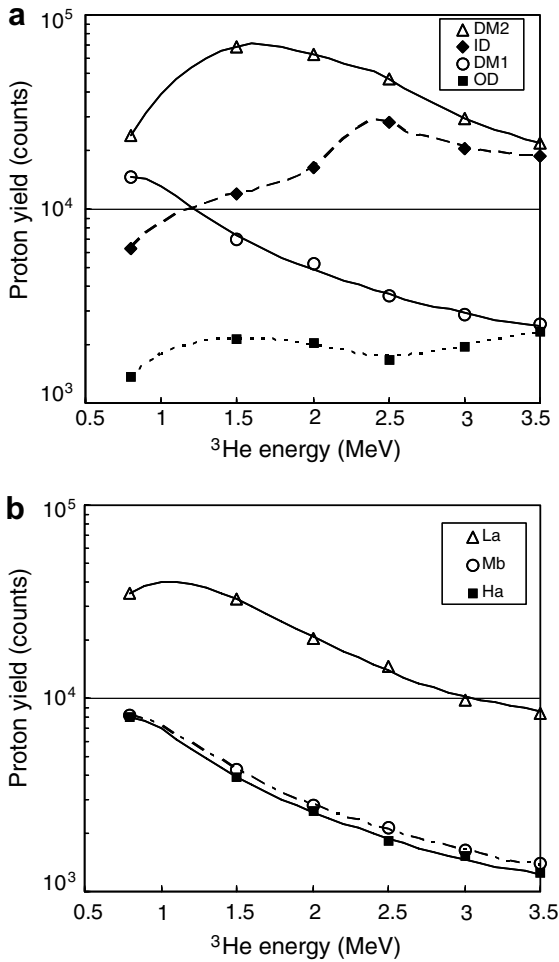


Fig. 3. Measured (points) and calculated (lines) proton yields for calculated D profile, as a function of the applied ^3He energy at (a) the divertor region and (b) the first wall samples.

the D depth profiles obtained by the SIMNRA program for (a) the divertor and (b) the first wall samples. The analyzed depth was 14×10^{23} carbon atoms/m², corresponding to a linear depth of 16.4 μm for carbon materials used for divertor target tiles with the density of 1.7 g/cm³. As described above, however, the density of the redeposited layers was 0.91 g/cm³. Thus, the depth of 14×10^{23} carbon atoms/m² corresponds to a linear depth of 30.7 μm for redeposited layers on the ID sample (see Table 1).

In the divertor region, the highest D/C ratio was found to be 0.07 in the outer dome wing tile (DM2) at a depth of 2×10^{23} carbon atoms/m². Deuterium tends to accumulate in the dome area, because the temperature of the tiles in the dome area (~ 800 K) is lower than that of the divertor target tiles as men-

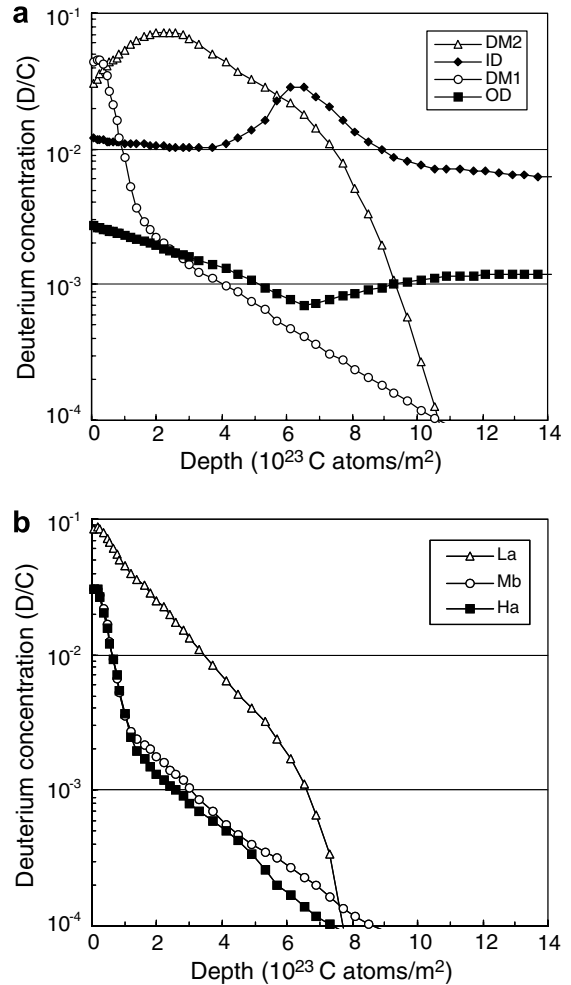


Fig. 4. Deuterium depth profiles obtained by using SIMNRA program at (a) the divertor and (b) the first wall samples.

tioned in the Section 2.1. In Fig. 4(a), the D depth profile shows a broad peak at a depth of 2×10^{23} C atoms/m² in the DM2 sample, there being redeposited layers of $0.45\text{--}1.4 \times 10^{23}$ C atoms/m² thickness on DM2. The D/C ratio in the near surface region (less than 0.5×10^{23} C atoms/m² thickness) of the DM2 was lower than that of the DM1 which is not covered with redeposited layers, but the D/C ratio of the deep region of DM2 was significantly larger than that of DM1. This indicates that D retained in the near surface regions of the redeposited layers during the D discharges was replaced isotopically by H during the H discharges owing to porous nature of the redeposited layers as appeared in less density.

On the other hand, in the inner divertor sample (ID), the D depth profile shows a broad peak at a

depth of 6×10^{23} C atoms/m². The thickness of the layer deposited on ID was 27×10^{23} C atoms/m². Comparing the thickness of the redeposited layers during H-discharges of less than 0.8×10^{23} C atoms/m² as described in the previous section, the D peak position was much deeper. In other words, the D depth profile does not show an interface between H-deposition and D-deposition layers in Fig. 4. These observations support that D retained in the shallow region of the redeposited layers was removed by H discharges, while D retained in the deeper region could not be removed [14], indicating that the H discharge is effective in removing the D trapped in the surface region (less than $\sim 5 \times 10^{23}$ C atoms/m²) of the deposition layer.

Fig. 5 compares deuterium retention for all samples determined by NRA. The gray and black bars indicate the integrated retention within the thickness of 14×10^{23} and 1×10^{23} C atoms/m², respectively. The amount of retained D in the outer dome wing tile (DM2) of 3.2×10^{22} was about two times larger than that in the inner divertor (ID), 1.7×10^{22} D atoms/m². But this does not mean the total D retention in ID is smaller than that in DM2, because the former had much thicker redeposited layers well beyond the analyzing depth of the present NRA analysis. In other words the D concentration in the redeposited layers on DM2 was larger than that on ID, because the temperature of the DM2 was lower than ID as already discussed above.

In the case of the outer divertor target (OD), the D/C ratio was very low (<0.003) even near the sur-

face. This can be attributed to the highest temperature of OD, ~ 1400 K, compared to that of ID (~ 1000 K). It is also notable that deuterium penetrates quite deep, though the concentration was quite low, suggesting molecular deuterium uptake in deeper region owing to high temperature.

3.3. Deuterium depth profiles in the first wall area and the dome top tile

In the first wall region shown in Fig. 4(b), the highest D/C ratio was found to be 0.09 in the upper region of the vacuum vessel (La). In this area, deposition was not appreciable. However, some carbon particles were accumulated along with deuterium, because the minimum distance between the last closed flux surface and the first wall surface on the upper region was maintained to be about 4 cm, expecting that there would be carbon deposition due to transport of the SOL plasma [15]. The temperature of the first wall region was lower than the divertor region. Consequently, more deuterium was retained in the first wall sample. In the case of the inner and outer middle height samples (Mb and Ha), the highest D/C ratio was 0.03 in the near surface region. The depth profiles were similar with each other. Any continuous redeposited layer was not observed on the surfaces of these samples.

The D depth profiles of the DM1, Mb and Ha samples were similar in Fig. 4(a) and (b). In JT-60U, NBI heating was conducted during plasma discharges. The energetic deuterons caused by deuterium NBI were implanted into the DM1 with high heat flux, and into the first wall region with low heat flux [6]. Therefore, the D retention value of DM1 was larger than the first wall samples (Mb and Ha) as shown in Fig. 5. During H discharges, the energetic protons produced by hydrogen NBI were also implanted. The projected range of proton transfer is shorter than that of deuterium at the same energies [6]. Consequently, D trapped close to the surface at depths less than 0.3×10^{23} C atoms/m² in the DM1 sample as shown in Fig. 4(a), was also replaced by the energetic protons produced by hydrogen NBI during hydrogen discharges.

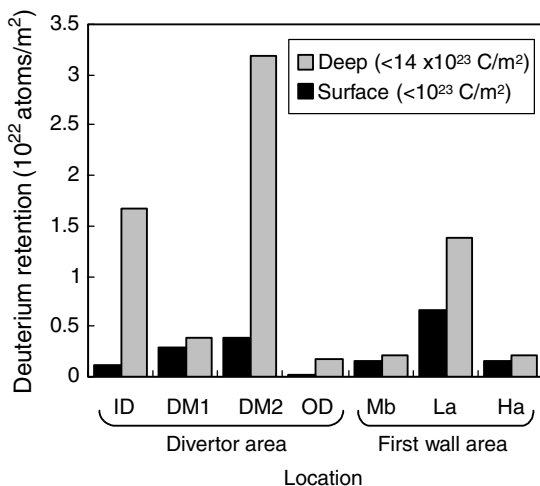


Fig. 5. Distribution of deuterium retention values obtained by NRA.

4. Conclusions

Depth profiles of deuterium embedded in graphite tiles of JT-60U were determined based on the $D(^3\text{He}, p)^4\text{He}$ resonant nuclear reaction caused by

^3He of different energies. The deuterium retention in tiles covered with redeposited carbon layers was high. In the divertor region, the high D/C of 0.07 was found in the outer dome wing tiles, but their D/C decayed rapidly with the depth corresponding to the thickness of the redeposited layers.

In the thick redeposited layers on the inner divertor target tile, the depth profile shows a broad peak in the deep region at a depth of 6×10^{23} C atoms/m² with nearly constant concentration well beyond the present analyzing depth. This indicates that the trapped D in the shallow region was removed by H discharges due to isotope exchange.

The outer divertor target tile showed the lowest D/C, less than 0.003 owing to its highest temperature.

The first wall tiles show similar depth profile to that for the dome top tile, i.e., D was trapped in the near surface region with high concentration but decayed rapidly with the depth. It is most likely that D was accumulated due to the implantation of energetic deuterons caused by deuterium NBI. The highest D/C ratio of 0.09 was found in the upper region of the first wall.

Acknowledgements

The present authors wish to thank Mr J. Dorner and Mr M. Fußeder for their technical assistance with the ^3He beam analyses. This work was carried out as an IPP–JAEA collaboration, and was a joint research effort between Japanese Universities and JAEA. We would like to thank the JT-60 team for their contribution to the operation and the experimental setup of JT-60U. The portion of the cal-

culational performed at the Institute of Physical Chemistry, Moscow, was supported by the ISTC under Project # 2805.

References

- [1] G. Federici, C.H. Skinner, J.N. Brooks, et al., Nucl. Fusion 41 (12R) (2001) 1967.
- [2] J.P. Coad, N. Bekris, J.D. Elder, et al., J. Nucl. Mater. 290–293 (2001) 224.
- [3] T. Tanabe, K. Miyasaka, K. Masaki, et al., J. Nucl. Mater. 307–311 (2002) 1441.
- [4] K. Masaki, K. Sugiyama, T. Hayashi, et al., J. Nucl. Mater. 337–339 (2005) 553.
- [5] H. Hirohata, T. Tanabe, T. Shibahara et al. Presented at 12th Int. Conf. on Fusion Reactor Mater., Santa Barbara, 2005, J. Nucl. Mater., in press.
- [6] T. Hayashi, K. Ochiai, K. Masaki, et al., J. Nucl. Mater. 349 (2006) 6.
- [7] T. Shibahara, T. Tanabe, Y. Hirohata, et al., J. Nucl. Mater. 357 (2006) 115.
- [8] Y. Gotoh, T. Tanabe, Y. Ishimoto, et al., J. Nucl. Mater. 357 (2006) 138.
- [9] M. Mayer, SIMNRA User's Guide, Tech. Report IPP 9/113, Max-Planck-Institut für Plasmaphysik, Garching, Germany, 1997.
- [10] M. Mayer, in: J.L. Duggan, I. Morgan (Eds.), Proc. of the 15th Int. Conf. on the Application of Accelerators in Research and Industry, AIP Conf. Proc., vol. 475, American Institute of Physics (1999). p. 541.
- [11] V.Kh. Alimov, M. Mayer, J. Roth, Nucl. Instrum. and Meth. B 234 (2005) 169.
- [12] Y. Gotoh, J. Yagyu, K. Masaki, et al., J. Nucl. Mater. 313–316 (2003) 370.
- [13] Y. Ishimoto, Y. Gotoh, T. Arai, et al., J. Nucl. Mater. 350 (2006) 301.
- [14] T. Shibahara, T. Tanabe, Y. Hirohata, et al., Nucl. Fusion 46 (2006) 841.
- [15] Y. Ishimoto, Y. Gotoh, T. Arai et al. Presented at 12th Int. Conf. on Fusion Reactor Mater., Santa Barbara, 2005, J. Nucl. Mater., in press.